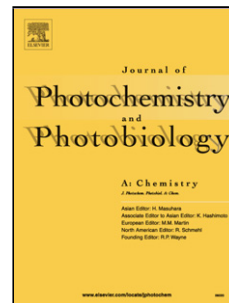


Accepted Manuscript

Title: Synthesis of novel colorants for DSSC to study effect of alkyl chain length alteration of auxiliary donor on light to current conversion efficiency

Authors: Manoj M Jadhav, Jayraj V. Vaghasiya, Dinesh Patil, Saurabh S. Soni, Nagaiyan Sekar



PII: S1010-6030(19)30004-8
DOI: <https://doi.org/10.1016/j.jphotochem.2019.03.043>
Reference: JPC 11780

To appear in: *Journal of Photochemistry and Photobiology A: Chemistry*

Received date: 3 January 2019
Revised date: 13 March 2019
Accepted date: 26 March 2019

Please cite this article as: Jadhav MM, Vaghasiya JV, Patil D, Soni SS, Sekar N, Synthesis of novel colorants for DSSC to study effect of alkyl chain length alteration of auxiliary donor on light to current conversion efficiency, *Journal of Photochemistry and Photobiology, A: Chemistry* (2019), <https://doi.org/10.1016/j.jphotochem.2019.03.043>

This is a PDF file of an unedited manuscript that has been accepted for publication. As a service to our customers we are providing this early version of the manuscript. The manuscript will undergo copyediting, typesetting, and review of the resulting proof before it is published in its final form. Please note that during the production process errors may be discovered which could affect the content, and all legal disclaimers that apply to the journal pertain.

Synthesis of novel colorants for DSSC to study effect of alkyl chain length alteration of auxiliary donor on light to current conversion efficiency

Manoj M Jadhav¹, Jayraj V. Vaghasiya^{2,3}, Dinesh Patil¹, Saurabh S. Soni^{2*}, Nagaiyan Sekar^{1*}

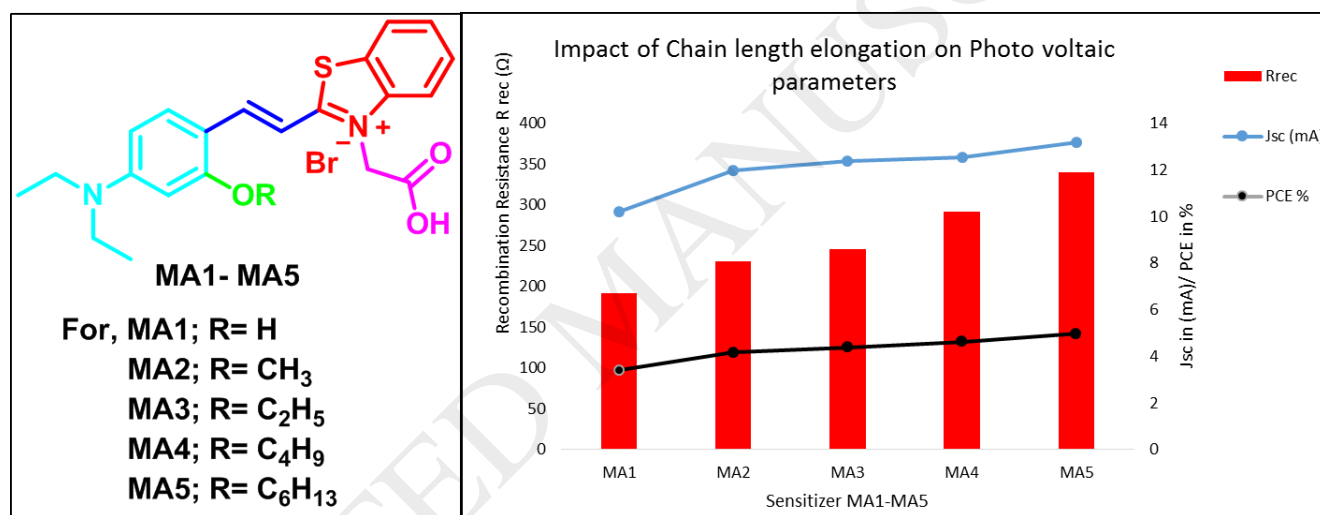
¹Department of Dyestuff Technology, Institute of Chemical Technology, N. P. Marg, Matunga, Mumbai, Maharashtra 400019, India

²Department of Chemistry, Sardar Patel University, Vallabh Vidyanagar, 388120, India

³Department of Materials Science and Engineering, National University of Singapore, 9 Engineering Drive 1, 117575, Singapore

*Authors for correspondence e-mail: nethi.sekar@gmail.com, soni_b21@yahoo.co.in

Graphical Abstract



Highlights

- Five hemicyanine based donor- π -acceptor chromophore having different alkyl chain length are made for DSSCs.
- Photophysical properties were studied using spectroscopic techniques and correlated with DFT studies.
- Structural modification are carried out to study the impact of chain length on properties of chromophores.
- Chain length has no impact on absorption and emission and HOMO-LUMO energy levels molar extinction coefficient decrease.
- Longer chain length results in enhancement in recombination resistance which increase the efficiency.
- The chromophore MA5 shows the highest efficiency of 4.97%.

Abstract:

Five (MA1-MA5) hemicyanine based sensitizer having N, N-diethyl aniline as a primary donor and hydroxy or alkoxy as an auxiliary donor have been synthesized to establish a correlation between amphiphilic nature of the sensitizer and charge recombination. A strong electron withdrawing 3-(carboxymethyl)-2-methylbenzo[d]thiazol-3-ium bromide has been explored as an acceptor. All the dyes were characterized by $^1\text{H-NMR}$, $^{13}\text{C-NMR}$ and CHN analysis. The photophysical properties of these dyes were recorded in seven different solvents which do not show any significant impact on absorption and emission maxima while molar absorptivity coefficient decreases with increase in alkyl chain length. These dyes show very poor emission in all the solvents. Nano-crystalline mesoporous TiO_2 based dye-sensitized solar cells were fabricated using MA1 to MA5 sensitizers to evaluate their photovoltaic performance. MA5 having six carbon alkyl chain shows maximum efficiency of 4.97% while MA1 without any alkyl chain shows the lowest efficiency of 3.40%. As the length of alkyl chain increase efficiency increase due to increment in short circuit current (J_{sc}) and retardation in the recombination process. Density functional theory (DFT) and time-dependent density functional theory (TD-DFT) were explored to obtain vertical excitation, HOMO-LUMO energy and electron density distribution.

Keywords:

DSSCs, Alkyl chain elongation, recombination resistance, DFT, TD-DFT

1. Introduction:

An organic based dye-sensitized solar cell (DSSCs) have become one of the most promising alternatives for the conventional silicon-based solar cell[1]. In 1991 Grätzel and co-workers have reported first ruthenium based DSSCs having good light to current conversion efficiency[2]. The sensitizer is an important aspect of DSSCs which plays a very crucial role in light harvesting[3–6]. The traditional ruthenium based sensitizers have shown mammoth success with high performance in DSSC[7–10]. These ruthenium based sensitizers suffer from heavy metal toxicity[11], environmental issues[12], high cost[13], and difficulty in purification[14]. The metal free organic sensitizer have been explored extensively in recent times[15–20] due to their low synthesis cost[21], environmental friendliness[22], high molar absorptivity[23,24], easily tuneable electrochemical properties[25] and established synthetic protocol[26]. Ideally, efficient organic sensitizer contains donor- π -acceptor (D- π -A) kind of skeleton having LUMO energy level above the conduction band of TiO₂ for efficient electron injection and HOMO energy level below the redox potential of electrolyte for effective dye regeneration[27–31]. These metal-free sensitizers show poor light to current conversion efficiency due to absorption in a narrow region, poor dye regeneration, high recombination rate, and dye aggregation. The dye aggregation arises due to pi-pi stacking of dye molecules. The drawback of dye aggregation is avoided by using alkyl chain which affects the planarity of the molecule. The length and position of the chain can play a vital role in governing the efficiency of the sensitizer in DSSCs. In recent years, researchers have systematically investigated the photoelectric conversion properties of hemicyanine dyes due to their D- π -A type of configuration[32]. The hemicyanine dyes have a strong acceptor group which can withdraw electron density from donor very efficiently due to positive charge present on the nitrogen atom, have high molar extinction coefficient and low emission. [33] These dyes show poor light to current conversion efficiency due to the narrow absorption spectrum, poor dye regeneration, charge separation and high recombination. In this paper, we have explored five sensitizers having varying length

of alkyl chain on an auxiliary donor to study the effect of alkyl chain variation on the performance of DSSCs. 2-Methylbenzo[d]thiazole is N-alkylated with bromoacetic acid is utilized as hemicyanine based acceptor over conventional acceptor to get dyes having strong electron withdrawing group, high molar extinction coefficient and low emission while *N,N*-diethylaniline along with hydroxy or alkoxy group are utilized as primary and auxiliary donor respectively. The strong electron donating group with alkoxy auxiliary donor with varied alkyl chain help to reduce dye aggregation and increase excited electron injection on TiO₂. The newly synthesized molecules have been characterized by ¹H NMR, ¹³C NMR, and elemental analyses. The electronic and photophysical properties of novel sensitizers have been studied and correlated with vertical excitation obtained by DFT. These dyes have been used to DSSC fabrication and their photovoltaic performance was investigated and a correlation between alkyl chain modification and its impact on cell performance is established. The introduction of alkyl chain has helped to overcome problem related to poor dye regeneration and high recombination.

<< Please insert Figure 1: Chemical structure of hemicyanine dyes MA1 to MA5.>>

<< Please insert Scheme 1: Synthesis of MA1 to MA5 >>

2. Experimental Section

2.1. Computational methods:

Density functional theory (DFT) was extensively utilized to optimize MA1 to MA5 in gas phase and six different solvents. A well-known B3LYP function [34] which is a combination of Becke's three parameter exchange functional (B3)[35] with the nonlocal correlation functional by Lee, Yang, and Parr (LYP)[36] was employed for optimization of molecules. The local minimum energy and vertical excitation of each compound is estimated using time dependent density functional theory (TD-DFT) calculation [37] at 6-31G+(d) basis set. The polarizable continuum model (PCM)[38,39] was employed for optimization in solvents. All electronic structure computations were carried out using the Gaussian 09 [40] program.

2.2. Chemicals and Instruments:

All the synthetic grade chemicals, reagents and solvents were procured from S. D. Fine Chemicals Pvt Ltd and used without purification. The 3-methoxy propionitrile (MNP), titania (IV) isopropoxide, LiI, Iodine (I₂), 4-tert-butyl pyridine (TBP), TiO₂ nanoparticle (<25nm particle size), ethyl cellulose and α -terpineol were purchased from the Sigma-Aldrich, India and used as it is without further purification. FTO doped transparent conducting

glass (12 Ω , Solaronix, thickness 2.2mm, SA, Switzerland) and Meltronix tape (20 μ m) were used for the fabrication of DSSC device. All the reactions were monitored by using 0.25 mm silica gel 60, F254 percolated TLC plates and visualized under UV light. $^1\text{H-NMR}$ and $^{13}\text{C-NMR}$ spectra were recorded on VARIAN 500-MHz instrument (USA) using TMS as an internal standard. Perkins-Elmer Lambda 25 spectrometer was used to record the UV-visible absorption spectra of the compounds in different solvents. Fluorescence emission spectra was recorded on Varian Cary Eclipse fluorescence spectrophotometer. Electrochemical Impedance Spectroscopy (EIS) were executed by utilizing Solartron 1260+1287 interfaces. CorrView and Zplot software were used for interpretation of data. EIS was measured by changing the frequency from 120 kHz to 0.1 Hz having an AC amplitude of 10 mV. Potentiometric data of all the samples estimated by doing cyclic voltammetry (CV) of all the samples electrochemical workstation (CHI660E, USA). A solution of 0.1 M tetra-n-butylammonium hexafluorophosphate dissolved in oxygen-free acetonitrile employed as supporting electrolyte. Three electrode system, in which porous glassy carbon electrode acting as a working electrode, thin wire of platinum acting as a counter electrode and Ag/AgCl acting as a reference electrode were utilized to construct the electrochemical cell. The photocurrent density to voltage (J–V curve) spectra were recorded by employing an external potential bias to the device. The generated photocurrent was measured with a Keithley 2450 digital source meter. Xenon lamp (solar simulator, PET, USA) calibrated with the light intensity 100mW.cm $^{-2}$ at AM 1.5 G solar light conditions by a certified silicon solar cell was used as light source. The photovoltaic parameters such as short-circuit current density (Jsc), open circuit voltage (Voc), fill factor (FF) and photo-conversion efficiency were calculated using previously reported method (refer experimental section in supporting information)[41,42]. Electron lifetime curves and Tafel polarization were obtained by using Solartron (1260) electrochemical analyzer with sweeping potential at $\pm 0.65\text{V}$ in dark with 25mV/s scan rate.

2.3 DSSC device Fabrication:

TiO $_2$ photoelectrode as a working electrode and platinized electrode as a counter electrode were utilized for fabrication of sandwich type DSSC device [43]. For TiO $_2$ photoelectrode a thin transparent layer of TiO $_2$ (18 NRT, Dyesol) with thickness 12 μ m was employed on FTO glass plate. The thickness of TiO $_2$ layer was measured by using a profilometer of Veeco Dektak 150 Stylus surface profiler. The photoelectrode was immersed overnight in an ethanol solution containing 3 mM dye solution for dye adsorption on the surface. The electrolytic solution of I $^-$ /I $_3^-$ prepared by dissolving 0.5M lithium iodide (LiI), 0.05 M Iodine (I $_2$), 0.5 M tert-butyl pyridine (TBP), and

0.5M guanidium thiocyanate (GSCN) in 3-methoxy propionitrile. The electrolyte was employed in the cell through the predrilled back holes onto the Pt-counter electrode. An epoxy adhesive was used to seal the holes. The DSSCs device was stored in dark at room temperature for 12 h before photovoltaic measurements. Active areas of the DSSCs were set to 0.16 cm² using a metal mask during the measurement of photovoltaic characterizations.

3. Results and Discussion

3.1. Design and synthesis of dyes

In order to understand the effect of chain length elongation on photovoltaic properties, we have synthesized five molecules MA1 to MA5 with varying the chain length from zero carbon chain in MA1 to Six carbon chain in MA5. Hemicyanine based dyes show narrow absorption, poor dye regeneration and high rate of recombination, but MA1 as reported in literature shows broad absorption spectrum when adsorbed on TiO₂ surface. This broad adsorption is due to the formation of aggregates and interaction of hydroxy group and TiO₂ to form new species which results in a red shift in absorption. It also shows a reduction in emission intensity in the presence of colloidal TiO₂[44] which can be very useful for enhanced light harvesting. By taking this into consideration we have synthesized MA1-MA5 where MA1 is used as the reference for comparing the impact of O-alkylation and chain length elongation on photovoltaic properties specially kinetic associated with dye recombination. Scheme 1 demonstrates the synthetic approach for the five dyes. Synthetic details and spectra data of all the compounds are given in supporting information. Synthesis of MA1 is carried out according to reported protocol[44,45]. The O-alkylation of 4-(diethylamino)-2-hydroxybenzaldehyde was carried out by refluxing it with a respective alkyl halide in toluene and sodium hydroxide using phase transfer catalyst (*p*-toluene sulphonic acid). 2-aminobenzenethiol and acetyl chloride were condensed with each other in toluene at reflux temperature to get 2-methylbenzo[d]thiazole which is further refluxed with bromoacetic acid in toluene to get acceptor 3-(carboxymethyl)-2-methylbenzo[d]thiazol-3-ium bromide (compound 6). Synthesized aldehyde and acceptor were condensed in acetonitrile using piperidine as a base to get crude MA1 to MA5 which is further purified using column chromatography. The systematic alteration of chain length on hydroxy group shows its impact on photophysical and photovoltaic properties due to change in band gap, charge separation and charge recombination.

3.2. Photophysical properties

Figure 2-6 represents the absorption and emission spectra of MA1-MA5 (1×10^{-6} M) recorded in seven solvents having different polarity and respective photophysical data is reproduced in Table 1-5. The quantum yield for MA1-MA5 in seven solvents are estimated by using Rhodamine 6G as standard [46,47]. For MA1 lowest absorption maxima of 516 nm observed in acetonitrile while highest absorption maxima of 560 nm have been observed in DCM. Increase in solvent polarity shows random solvatochromism in case of MA1. MA1 shows exceptional behavior in non-polar DCM solvent where it shows highest absorption maxima and the highest molar absorptivity ($94000 \text{ mol}^{-1} \text{ cm}^{-1}$). MA1 shows lowest emission maxima at 577 nm in acetonitrile whereas the highest emission maximum of 588 nm was observed in DMSO. MA1 shows a low Stokes shift ranging from 26 nm to 61 nm. The lowest Stokes shift of 26 nm is observed in DCM while the highest Stokes shift of 61 nm was observed in acetonitrile. In MA2, where a hydroxy group is replaced by O-methyl shows a red shift in absorption and emission. The redshift is due to the positive inductive effect caused by the methyl group which improves the donating capacity of dye suggesting the role of methoxy as auxiliary donor[20]. MA2 shows lowest absorption maxima of 531 nm in acetonitrile while highest absorption maxima of 564 nm was observed in dichloromethane. The lowest emission maxima of 583 nm was observed in ethanol and acetone while the highest emission maxima of 593 nm was observed in dimethyl sulfoxide (DMSO). MA2 shows poor molar extinction coefficient in ethyl acetate which might be due to its poor solubility in these solvents. For MA3 where O-ethyl group is incorporated, absorption maxima range from 524 nm to 558 nm while emission maxima range from 578 nm to 607 nm. MA3 show poor molar extinction coefficient in ethyl acetate and acetone which is due to its poor solubility. In case of MA4 where the o-butyl group is introduced and MA5 where the o-hexyl group is introduced absorption maxima range from 530 nm to 559 nm and 525 nm to 554 nm respectively. For MA4 emission maxima lie in the range of 564 nm to 596 nm while for MA5 it lies in the range of 588 nm to 598 nm. Nearly the same absorption and emission maxima of MA2-MA5 suggest the zero impact of chain length elongation on photophysical behavior. The comparison of experimental absorption along with vertical excitation obtained by TD-DFT in respective solvents is replicated in supporting **Table S1-S5**. The vertical excitation obtained from TD-DFT calculation are comparable with observed absorption. The orbital contribution for all the vertical excitation lies in the range of 98.8 to 99.5%. Table 6 represents the absorption-emission data and vertical excitation of sensitizer **MA1 to MA5** in acetonitrile. From Table 6 it is evident that the introduction of alkyl chain

shows a very minute bathochromic shift in absorption and emission while chain length elongation does not have any significant impact on absorption and emission maxima. The results further suggest that as the chain length increases molecular weight increase and molar absorptivity decrease as the alteration in chain length is not contributing to electron conjugation. The absorption and emission spectra of dye adsorbed on nanocrystalline TiO₂ surface is given in supporting information (Figure S1). When anchored on titania, a slight blue shift of absorption maxima and widening of the absorption spectrum was found as compared to absorption in solution is observed. The increase in the chain do not show any significant impact on absorption maxima but shows enhancement in intensity of absorbed light and widening of the absorption spectrum. MA1-MA5 do not show any emission on TiO₂ surface due to quenching of emission intensity.

<< Please insert Figure 2: Absorption and emission spectra of MA1 (1*10⁻⁶ M).>>

<< Please insert Figure 3: Absorption and emission spectra of MA2 (1*10⁻⁶ M).>>

<< Please insert Figure 4: Absorption and emission spectra of MA3 (1*10⁻⁶ M).>>

<< Please insert Figure 5: Absorption and emission spectra of MA4 (1*10⁻⁶ M).>>

<< Please insert Figure 6: Absorption and emission spectra of MA5 (1*10⁻⁶ M).>>

<< Please insert Table 1: Photo physical data for MA1. >>

<< Please insert Table 2: Photo physical data for MA2. >>

<< Please insert Table 3: Photo physical data for MA3. >>

<< Please insert Table 4: Photo physical data for MA4. >>

<< Please insert Table 5: Photo physical data for MA5. >>

<< Please insert Table 6: Photophysical properties of MA1-MA5 in Acetonitrile (1.0*10⁻⁶M). >>

3.3. Electrochemical properties:

Cyclic voltammetry measurement was carried out to estimate oxidation and reduction potential of MA1 to MA5 sensitizer and cyclic voltammogram of MA1 to MA5 is reproduced in Figure 7. The pronounced oxidation wave observed in cyclic voltammogram attributing to removal of an electron from the lone pair of nitrogen atom has been utilized to estimate E_{onset} value. The first oxidation potential E_{HOMO} value is calculated from the following equation:

$$E_{HOMO} = - (E_{onset} - (Ag/Ag^+) + 4.8) \text{ eV} \text{-----(a)}$$

The excited state oxidation potentials (E_{LUMO}) is obtained from the following eq:

$$E_{LUMO} = E_g - E_{HOMO} \text{-----(b)}$$

Where, E_g is the optical band gap obtained from absorption spectra of the dye in acetonitrile. The oxidation-reduction potential values obtained from cyclic voltammogram are replicated in Table 7. The first oxidation potential E_{HOMO} obtained from equation (a) is more positive than the redox potential of redox couple of electrolyte (I^-/I_3^-) which suggest the feasibility of transfer of electron from electrolyte to oxidised dye to promote reduction of dye. The excited state oxidation potential E_{LUMO} has more negative values than the conduction band of TiO_2 which suggest the possibility of transfer of electron from LUMO level of oxidised dye onto the conduction band of TiO_2 . Table 8 represents the HOMO-LUMO energy levels obtained from optimised structures using DFT. These values shows very good correlation with experimental values. Figure 8 gives the pictorial representation of HOMO-LUMO energy levels obtained by DFT and cyclic voltammogram. From Figure 8 it is evident that elongation of alkyl chain is not having any significant effect on HOMO-LUMO energy levels as alkyl chain is not altering the electron density as evident from pictorial presentation of electron density at HOMO-LUMO energy level (Figure 8). Also from UV-Visible study it is clear that the chain alteration dose not contribute to overall conjugation in the sensitizers, hence no significant change in HOMO-LUMO energy level is observed.

<< Please insert Figure 7: Absorption and emission spectra of MA5 (1*10⁻⁶ M).>>

<< Please insert Table 7: Oxidation-reduction potential of MA1-MA5 in acetonitrile obtained by cyclic voltammetry. >>

<< Please insert Table 8: HOMO and LUMO energy values in eV for MA1 to MA5 in acetonitrile obtained from optimized geometry. >>

<< Please insert Figure 8: Comparative analysis of HOMO-LUMO energy levels obtained by Cyclic voltammetry and DFT.>>

Figure 9. represents the pictorial representation of electron density at HOMO-LUMO level in MA1 to MA5. For MA1 at HOMO level electron density lies mainly on nitrogen and oxygen atom in donor moiety and a sulphur atom in acceptor moiety while it shifts slightly to the nitrogen atom of benzothiazole upon excitation at LUMO level. This signifies the charge transfer from donor to positively charge hemicyanine nitrogen. For MA1 to MA5

the electron density distribution at HOMO-LUMO level is similar which suggest the zero impact of alkyl chain elongation on electron density.

<< Please insert **Figure 9: Pictorial presentation of electron density distribution at HOMO and LUMO in MA1 to MA5.**>>

3.4. Photovoltaic properties of DSSC

Preliminary results based on photophysical properties and cyclic voltammetry data shows that the dyes MA1 to MA5 have suitable ground/excited state oxidation potentials for their application as sensitizers for conventional DSSCs. LUMO energy levels for these dyes are sufficiently negative for electron injection of excited dye on TiO₂ and HOMO energy level are sufficiently lower than redox potential of electrolyte for dye regeneration. The molar absorptivity of the sensitizer decreases from MA1 to MA5 as chain length increases. While cyclic voltammetry, DFT analysis and electron density analysis show no impact on chain elongation. Based on these results one can predict a decrease in light to photocurrent conversion efficiency from MA1 to MA5. The photovoltaic parameters of the freshly fabricated cells containing MA1 to MA5 as sensitizer are measured under AM1.5 solar irradiation (100 mW cm⁻²) and the corresponding *J-V* characteristics graph of all cell are replicated in **Figure. 10 (a)**. The photovoltaic parameters such as short-circuit current density (*J_{sc}*), open-circuit voltage (*V_{oc}*), fill factor (*FF*) and overall conversion efficiency (*η*) are tabulated in **Table 9**. The results clearly suggest the importance of alkyl chain length on performance of dye as sensitizers in DSSCs. Taking **MA1** as a standard prototype, **MA2 to MA5** molecules were designed and synthesized in to understand the significance of alkyl chain modification of auxiliary donor on light to the current conversion efficiency of DSSCs. MA1 shows the lowest light to the current conversion efficiency of 3.40% in the series. The low efficiency of MA1 is due to low *J_{sc}* which is 10.20mA/cm² which in turn has affected the *P_{max}*. In MA2 we have carried out o-methylation at donor. This methoxy group affects the short circuit current significantly leading to an increase in *J_{sc}* value to 11.96 mA/cm² which leads to improvement in efficiency to 4.17% which is 22.6% more than MA1. In case of MA3, the length of O-alkyl chain has been increased by CH₂ in comparison with MA2 which results in 5.3% enhancement in efficiency. The photocurrent efficiency of MA3 is 4.39%. Subsequent enhancement in alkyl chain length in MA4 and MA5 has resulted in enhancement in photocurrent efficiency due to steady growth in short circuit current. MA4 shows the efficiency of 4.62% with *J_{sc}* of 12.54mA/cm² while MA5 shows the efficiency of 4.97% with *J_{sc}* of 13.18mA/cm². In the year 2005, Bao-Wen Zhang and co-workers have reported 5.2% efficiency [46] of MA1

whereas we have got 3.31% efficiency in our lab. The lower efficiency might be due to the difference in cell fabrication process employed in our lab. Under the same conditions, **MA2 to MA5** sensitized solar cells gave overall power conversion efficiencies (η) of 4.17%, 4.39%, 4.62%, and 4.97% respectively. This clearly suggests that the experimental efficiencies can be higher under improved conditions. The light to current conversion efficiency increases from MA1 to MA5 clearly suggesting the role of alkyl chain on the enhancement of efficiency.

<< Please insert Table 9: Photovoltaic properties of chromophores. >>

<< Please insert Figure 10: (a) Photovoltaic characterization (I-V spectra) MA1-MA5 and (b) Nyquist plots of DSSC devices fabricated using MA1-MA5 chromophores.>>

To clarify the UV Vis trend on TiO₂ film and influence of the alkyl chain length of the MA series dye on the device performance, we carried out IPCE (incident photo to current conversion efficiency) as a function of wavelength. As shown in supporting information **Figure S2**, MA-5 dye efficiency converts the light to current in the region from 300 to 710 nm. The highest IPCEs value of 49% at 510nm for MA5 dye. Meanwhile the IPCE for MA-1 and 2 are obviously lower at 400nm to 600nm, which is in accordance with their absorption spectra on the nanocrystalline TiO₂ film. To understand the impact of chain length alteration on the photovoltaic performance we have carried out electrochemical impedance spectral analysis. EIS was recorded with two-electrode alignment under forward bias in the dark light[47,48]. EIS spectra are given in Figure 10(b) while high-frequency range arc (R_{ct}), recombination resistance (R_{rec}) and constant phase element-parameter (CEP-P) values are determined from EIS spectra are replicated in Table 9. The high-frequency range arc is suppressed and can't be visualized clearly. The R_{ct} value lies in the range of 21.9 to 22.9 Ω which is almost constant for MA1 to MA5. CPE-P value suggests the surface unevenness and penetrability of the photoelectrode used in DSSCs is almost constant for all the devices and lies in the range of 0.79 to 0.82. As the length of alkyl chain increase from MA1 to MA5 the recombination resistance (R_{rec}) measured from EIS shows radical enhancement. MA1 shows lowest recombination resistance (192 Ω) suggesting the rate of electron transport via external circuit is low and rate of recombination is high which leads to regeneration of dye without transfer of electron through the external circuit. For MA5 recombination resistance is highest (340 Ω). The high recombination resistance suggest the ease of electron transport through an external circuit which generates a higher potential difference between two

electrodes. It is evident from EIS spectra that increase in alkyl chain length retards the electron recombination kinetic process which leads to enhancement in efficiency.

<< Please insert Figure 11: (a) Open Circuit Voltage Decay and (b) Electron carrier lifetime.>>

The impact of chain length alteration on open circuit voltage decay (OCVD) measured and decay in V_{oc} (V) against time (sec) replicated in Figure 11(a). Open circuit voltage decay measurement was carried out by estimating steady state voltage under 1 sun radiation and then decay measurement was carried out in dark by discontinuing the light radiation[49,50]. The steady state voltage is replicated in Table 9 which shows slight increment from MA1 to MA2. For MA1 V_{oc} is lowest i.e. 0.682V which increase up to 0.696V upon o-methylation. This further remains constant for MA3 and MA4 while for MA5 it increases to 0.712V. Open circuit voltage is highest for MA5. When the light radiation source is discontinued the open circuit voltage (V_{oc}) of the cells exhibit a sharp decline because of electron recombination. The decay of MA1 is very sharp in comparison with remaining dyes while MA5 shows steady decay in open circuit voltage. For the rest of the dyes, decay curve remains in-between. From OCVD spectra it is evident that introduction of O-alkylation has pronounced effect on open circuit voltage and increasing the chain length retards the open circuit voltage decay which inhibits the back recombination process in dark leading to an improved photovoltaic performance by improving the forward kinetic process. The electron-carrier lifetime (τ_n) for MA1 to MA5 is estimated by using below given equation[51] and electron carrier lifetime spectra is given in Figure 11(b).

$$\tau_n = \frac{K_B T}{e} \left(\frac{dV_{oc}}{dt} \right)^{-1}$$

The electron carrier lifetime for MA1 is lowest and shows sharp decay with an increase in potential while for MA5 it is highest. For MA2, MA3 and MA4 electron carrier lifetime lies in-between MA1 to MA5. CHI660E electrochemical workstation has been utilised to record Tafel polarization plot which is been replicated in Figure 12. Tafel polarization plot was recorded by employing DC potential from $\pm 0.65V$ by keeping 10 mV s^{-1} scan rate in dark to understand charge transmission of I^-/I_3^- redox couple on the titania surface[52–54]. The cathodic (α_c) and anodic (α_a) rate of reaction on TiO_2 electrode and I^-/I_3^- electrolyte interface can be defined by the following equation[55]

$$j = -j_0 \left(\exp^{\alpha_c n F / RT} (E - E_{eq}) - \exp^{\alpha_a n F / RT} (E - E_{eq}) \right)$$

Here, E is applied voltage while E_{eq} represents the equilibrium potential of the redox mediator. J_o represents current exchange density. In dark condition equation that $j = j_o$ as $E = E_{eq}$ and J_o depends on the concentrations of I^-/I^{3-} and reaction area on the titania surface. Figure. 11 shows Tafel polarization curve plotted to gain insight into the electrode kinetics for DSSCs based on the redox shutter. For all the chromophoric dyes the values of β_c and β_a current are depicted in Table 10. We can see the higher β_c value determine the reduced recombination reaction at counter/electrolyte interface, while lower values of β_a correspond to the enhanced reaction of iodide at the photoanode/electrolyte interface.

<< Please insert Figure 12: Tafel polarization plot.>>

4. Conclusion:

In this paper, we have reported synthesis, characterization, DFT and TD-DFT of five hemicyanine based sensitizer MA1 to MA5. All these compounds were successfully characterized using 1H NMR, ^{13}C NMR and elemental analysis. These sensitizers were explored for their potential application in DSSCs. The photo-physical behaviour of these compounds were studied in seven different solvents and successfully correlated with vertical excitation obtained by TD-DFT. Zero or negative impact of chain length elongation has been observed on photophysical, cyclic voltammetry and DFT study. In spite of this photovoltaic efficiency shows increment in efficiency with chain length elongation due to enhancement in recombination resistance as measured by EIS. This highlights the impact of chain length elongation. The order of power conversion efficiency for all sensitizers increases from MA1 to MA5.

Acknowledgement

Manoj M Jadhav is grateful to Department of Science and Technology (Government of India) and Technical Education Quality Improvement Programme, Ministry of Human Resource Development for financial support.

References:

- [1] Pashaei B, Shahroosvand H, Graetzel M, Nazeeruddin MK. Influence of Ancillary Ligands in Dye-Sensitized Solar Cells. Chem Rev 2016;116:9485–564. doi:10.1021/acs.chemrev.5b00621.

- [2] O'Regan B, Grätzel M. A low-cost, high-efficiency solar cell based on dye-sensitized colloidal TiO₂ films. *Nature* 1991;353:737–40. doi:10.1038/353737a0.
- [3] Wang ZL, Wu W. Nanotechnology-enabled energy harvesting for self-powered micro-/nanosystems. *Angew Chem Int Ed Engl* 2012;51:11700–21. doi:10.1002/anie.201201656.
- [4] Ladomenou K, Nikolaou V, Charalambidis G, Coutsolelos a G. Artificial hemes for DSSC and/or BHJ applications. *Dalt Trans* 2016;45:1111–26. doi:10.1039/c5dt03834k.
- [5] Wei D. Dye sensitized solar cells. *Int J Mol Sci* 2010;11:1103–13. doi:10.3390/ijms11031103.
- [6] Daniel P. Hagberg, Jun-Ho Yum, HyoJoong Lee, Filippo De Angelis, Tannia Marinado, Karl Martin Karlsson, Robin Humphry-Baker, Licheng Sun†, Anders Hagfeldt MG and MKN. Molecular engineering of organic sensitizers for dye-sensitized solar cell applications. *J Am Chem Soc* 2008;130:6259–6266. doi:10.1021/ja800066y.
- [7] Kong F-T, Dai S-Y, Wang K-J. Review of Recent Progress in Dye-Sensitized Solar Cells. *Adv Optoelectron* 2007;2007:1–13. doi:10.1155/2007/75384.
- [8] Grätzel M. Dye-sensitized solar cells. *J Photochem Photobiol C Photochem Rev* 2003;4:145–53. doi:10.1016/S1389-5567(03)00026-1.
- [9] Hagfeldt A, Boschloo G, Sun L, Kloo L, Pettersson H. Dye-sensitized solar cells. *Chem Rev* 2010;110:6595–663. doi:10.1002/chem.201101923.
- [10] Pavan Kumar C, Anusha V, Narayanaswamy K, Bhanuprakash K, Islam A, Han L, et al. New ruthenium complexes (Ru[3+2+1]) bearing π -extended 4-methylstyryl terpyridine and unsymmetrical bipyridine ligands for DSSC applications. *Inorganica Chim Acta* 2015;435:46–52. doi:10.1016/j.ica.2015.04.038.
- [11] Wu F, Zhao S, Lee LTL, Wang M, Chen T, Zhu L. Novel D- π -A organic sensitizers containing diarylmethylene-bridged triphenylamine and different spacers for solar cell application. *Tetrahedron Lett* 2015;56:1233–8. doi:10.1016/j.tetlet.2015.01.156.
- [12] Wang L, Shen P, Cao Z, Liu X, Huang Y, Liu C, et al. Effects of the acceptors in triphenylamine-based D-A'- π -A dyes on photophysical, electrochemical, and photovoltaic properties. *J Power Sources* 2014;246:831–9. doi:10.1016/j.jpowsour.2013.08.034.
- [13] Long J, Liu X, Guo H, Zhao B, Tan S. Effect of conjugated side groups on the photovoltaic performances of triphenylamine-based dyes sensitized solar cells. *Dye Pigment* 2016;124:222–31. doi:10.1016/j.dyepig.2015.09.025.
- [14] Gupta KS V, Singh SP, Islam A, Han L, M. C. Simple Fluorene Based Triarylamine Metal-Free Organic Sensitizers. *Electrochim Acta* 2015;174:581–7. doi:http://dx.doi.org/10.1016/j.electacta.2015.05.158.
- [15] Mishra A, Fischer MKR, Bäuerle P. Metal-free organic dyes for dye-sensitized solar cells: from structure:

- property relationships to design rules. *Angew Chem Int Ed Engl* 2009;48:2474–99. doi:10.1002/anie.200804709.
- [16] Panicker JS, Balan B, Soman S, Nair VC. Understanding structure-property correlation of metal free organic dyes using interfacial electron transfer measurements. *Sol Energy* 2016;139:547–56. doi:10.1016/j.solener.2016.10.007.
- [17] Chen C, Liao J-Y, Chi Z, Xu B, Zhang X, Kuang D-B, et al. Metal-free organic dyes derived from triphenylethylene for dye-sensitized solar cells: tuning of the performance by phenothiazine and carbazole. *J Mater Chem* 2012;22:8994–9005. doi:10.1039/c2jm30254c.
- [18] Tsao MH, Wu TY, Wang HP, Sun IW, Su SG, Lin YC, et al. An efficient metal-free sensitizer for dye-sensitized solar cells. *Mater Lett* 2011;65:583–6. doi:10.1016/j.matlet.2010.10.072.
- [19] Avhad K, Jadhav M, Patil D, Chowdhury TH, Islam A, Bedja I, et al. Rhodanine-3-acetic acid containing D- π -A push-pull chromophores: Effect of methoxy group on the performance of dye-sensitized solar cells. *Org Electron* 2019;65:386–93. doi:https://doi.org/10.1016/j.orgel.2018.11.041.
- [20] Jadhav MM, Vaghasiya JV, Patil DS, Soni SS, Sekar N. Structure-efficiency relationship of newly synthesized 4-substituted donor- π -acceptor coumarins for dye-sensitized solar cells. *New J Chem* 2018;42:5267–75. doi:10.1039/c7nj04954d.
- [21] Yang S, Liu J, Zhou P, Han K, He G. Photo-induced intramolecular charge transfer from antenna to anchor groups in phenoxazine dyes. *Chem Phys Lett* 2011;512:66–9. doi:10.1016/j.cplett.2011.06.088.
- [22] Chen Z, Li F, Huang C. Organic D- π -A Dyes for Dye-Sensitized Solar Cell. *Curr Org Chem* 2007;11:1241–58. doi:10.2174/138527207781696008.
- [23] Zhang G, Bala H, Cheng Y, Shi D, Lv X, Yu Q, et al. High efficiency and stable dye-sensitized solar cells with an organic chromophore featuring a binary p-conjugated spacer. *Chem Commun* 2009;0:2198–200. doi:10.1039/b822325d.
- [24] Ooyama Y, Harima Y. Molecular designs and syntheses of organic dyes for dye-sensitized solar cells. *European J Org Chem* 2009:2903–34. doi:10.1002/ejoc.200900236.
- [25] Liu X, Cao Z, Huang H, Liu X, Tan Y, Chen H, et al. Novel D-D- π -A organic dyes based on triphenylamine and indole-derivatives for high performance dye-sensitized solar cells. *J Power Sources* 2014;248:400–6. doi:10.1016/j.jpowsour.2013.09.106.
- [26] Cui Y, Wu Y, Lu X, Zhang X, Zhou G, Miapheh FB, et al. Incorporating Benzotriazole Moiety to Construct D- π -A Organic Sensitizers for Solar Cells: Significant Enhancement of Open-Circuit Photovoltage with Long Alkyl Group. *Chem Mater* 2011;23:4394–401. doi:10.1021/cm202226j.
- [27] Wang ZS, Cui Y, Dan-oh Y, Kasada C, Shinpo A, Hara K. Thiophene-functionalized coumarin dye for efficient dye-sensitized solar cells: Electron lifetime improved by coadsorption of deoxycholic acid. *J Phys*

- Chem C 2007;111:7224–30. doi:10.1021/jp067872t.
- [28] Fuke N, Fukui A, Islam A, Komiya R, Yamanaka R, Han L, et al. Electron transport in back contact dye-sensitized solar cells. *J Appl Phys* 2008;104:064307. doi:10.1063/1.2975182.
- [29] Cheng M, Yang X, Zhang F, Zhao J, Sun L. Tuning the HOMO and LUMO Energy Levels of Organic Dyes with N-Carboxomethylpyridinium as Acceptor To Optimize the Efficiency of Dye-Sensitized Solar Cells. *J Phys Chem C* 2013;117:9076–83. doi:10.1021/jp311378b.
- [30] Patil DS, Sonigara KK, Jadhav MM, Avhad KC, Sharma S, Soni SS, et al. Effect of structural manipulation in hetero-tri-aryl amine donor-based D-A'- π -A sensitizers in dye-sensitized solar cells. *New J Chem* 2018;42:4361–71. doi:10.1039/c7nj04620k.
- [31] Patil D, Jadhav M, Avhad K, Chowdhury TH, Islam A, Bedja I, et al. A new class of triphenylamine-based novel sensitizers for DSSCs: A comparative study of three different anchoring groups. *New J Chem* 2018;42:11555–64. doi:10.1039/c8nj01029c.
- [32] Wang ZS, Li FY, Huang CH. Photocurrent enhancement of hemicyanine dyes containing RSO₃- group through treating TiO₂ films with hydrochloric acid. *J Phys Chem B* 2001;105:9210–7. doi:10.1021/jp010667n.
- [33] Yao Q-H, Shan L, Li F-Y, Yin D-D, Huang C-H. An expanded conjugation photosensitizer with two different adsorbing groups for solar cells. *New J Chem* 2003;27:1277. doi:10.1039/b302552g.
- [34] Treutler O, Ahlrichs R. Efficient molecular numerical integration schemes. *J Chem Phys* 1995;102:346–54. doi:org/10.1063/1.469408.
- [35] Becke AD. A new mixing of Hartree–Fock and local density-functional theories. *J Chem Phys* 1993;98:1372–7. doi:org/10.1063/1.464304.
- [36] Lee C, Yang W, Parr RG. Development of the Colle-Salvetti correlation-energy formula into a functional of the electron density. *Phys Rev B* 1988;37:785–9. doi:10.1103/PhysRevB.37.785.
- [37] Casida ME, Jamorski C, Casida KC, Salahub DR. Molecular excitation energies to high-lying bound states from time-dependent density-functional response theory: Characterization and correction of the time-dependent local density approximation ionization threshold. *J Chem Phys* 1998;108:4439–49. doi:org/10.1063/1.475855.
- [38] Cossi M, Barone V, Cammi R, Tomasi J. Ab initio study of solvated molecules: a new implementation of the polarizable continuum model. *Chem Phys Lett* 1996;255:327–35. doi:http://dx.doi.org/10.1016/0009-2614(96)00349-1.
- [39] Tomasi J, Mennucci B, Cammi R. Quantum Mechanical Continuum Solvation Models. *Chem Rev* 2005;105:2999–3094. doi:10.1021/cr9904009.

- [40] Frisch MJ, Trucks GW, Schlegel HB, Scuseria GE, Robb MA, Cheeseman JR, et al. Gaussian 09, Revision D.01. 2013.
- [41] Hagfeldt A, Graetzel M. Light-Induced Redox Reactions in Nanocrystalline Systems. *Chem Rev* 1995;95:49–68. doi:10.1021/cr00033a003.
- [42] Hara K, Arakawa H, Dssc C, Grätzel M. Dye-sensitized Solar Cells. *J Photochem Photobiol C Photochem Rev* 2003;4:6595–663. doi:10.1016/S1389-5567(03)00026-1.
- [43] Vaghasiya J V, Sonigara KK, Prasad J, Beuvier T, Gibaud A, Soni SS. Role of a phenothiazine/phenoxazine donor in solid ionic conductors for efficient solid state dye sensitized solar cells. *J Mater Chem A* 2017;5:5373–82. doi:10.1039/C6TA09777D.
- [44] Chen Y-S, Li C, Zeng Z-H, Wang W-B, Wang X-S, Zhang B-W. Efficient electron injection due to a special adsorbing group's combination of carboxyl and hydroxyl: dye-sensitized solar cells based on new hemicyanine dyes. *J Mater Chem* 2005;15:1654–61. doi:10.1039/B418906J.
- [45] Tatay S, Gaviña P, Coronado E, Palomares E. Optical Mercury Sensing Using a Benzothiazolium Hemicyanine Dye. *Org Lett* 2006;8:3857–60. doi:10.1021/ol0615580.
- [46] Chen Y, Li C, Zeng Z, Wang W, Wang X. Efficient electron injection due to a special adsorbing group's combination of carboxyl and hydroxyl : dye-sensitized solar cells based on new hemicyanine dyes { 2005:1654–61. doi:10.1039/b418906j.
- [47] Vaghasiya J V, Sonigara KK, Beuvier T, Gibaud A, Soni SS. Iodine induced 1-D lamellar self assembly in organic ionic crystals for solid state dye sensitized solar cells. *Nanoscale* 2017;9:15949–57. doi:10.1039/C7NR06128E.
- [48] Raju TB, Vaghasiya J V, Afroz MA, Soni SS, Iyer PK. Influence of m-fluorine substituted phenylene spacer dyes in dye-sensitized solar cells. *Org Electron* 2016;39:371–9. doi:https://doi.org/10.1016/j.orgel.2016.10.024.
- [49] Vaghasiya J V, Sonigara KK, Patel MH, Patel VK, Sekar N, Soni SS. Low cost and efficient hetero-anthracene based small organic hole transporting materials for solid state photoelectrochemical cells. *Mater Today Energy* 2018;9:496–505. doi:https://doi.org/10.1016/j.mtener.2018.07.006.
- [50] Vaghasiya J V, Sonigara KK, Soni SS, Tan SC. Dual functional hetero-anthracene based single component organic ionic conductors as redox mediator cum light harvester for solid state photoelectrochemical cells. *J Mater Chem A* 2018;6:4868–77. doi:10.1039/C8TA00304A.
- [51] Zaban A, Greenshtein M, Bisquert J. Determination of the Electron Lifetime in Nanocrystalline Dye Solar Cells by Open-Circuit Voltage Decay Measurements. *ChemPhysChem* 2003;4:859–64. doi:10.1002/cphc.200200615.
- [52] Huo Z, Zhang C, Fang X, Cai M, Dai S, Wang K. Low molecular mass organogelator based gel electrolyte

- gelated by a quaternary ammonium halide salt for quasi-solid-state dye-sensitized solar cells. *J Power Sources* 2010;195:4384–90. doi:<http://dx.doi.org/10.1016/j.jpowsour.2009.12.107>.
- [53] Sonigara KK, Vaghasiya J V, Machhi HK, Prasad J, Gibaud A, Soni SS. Anisotropic One-Dimensional Aqueous Polymer Gel Electrolyte for Photoelectrochemical Devices: Improvement in Hydrophobic TiO₂–Dye/Electrolyte Interface. *ACS Appl Energy Mater* 2018;1:3665–73. doi:10.1021/acsaem.8b00444.
- [54] Vaghasiya J V, Nandakumar DK, Yaoxin Z, Tan SC. Low toxicity environmentally friendly single component aqueous organic ionic conductors for high efficiency photoelectrochemical solar cells. *J Mater Chem A* 2018;6:1009–16. doi:10.1039/C7TA09557K.
- [55] Petrii OA, Nazmutdinov RR, Bronshtein MD, Tsirlina GA. Life of the Tafel equation: Current understanding and prospects for the second century. *Electrochim Acta* 2007;52:3493–504. doi:<http://dx.doi.org/10.1016/j.electacta.2006.10.014>.

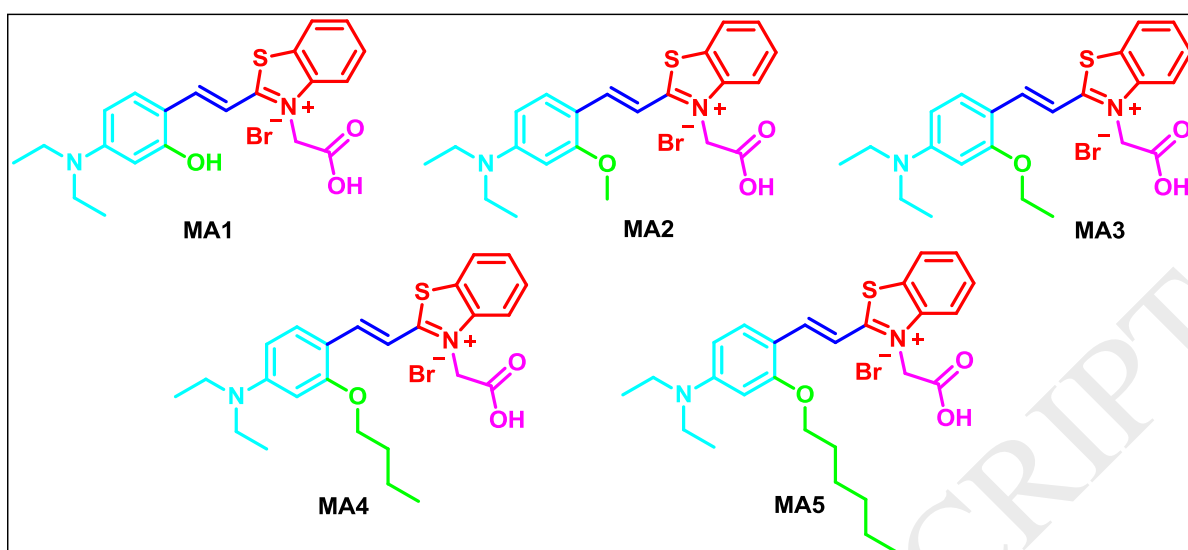


Figure 1 Chemical structure of hemicyanine dyes MA1 to MA5.

Figure 2: Absorption and emission spectra of MA1 (1×10^{-6} M)

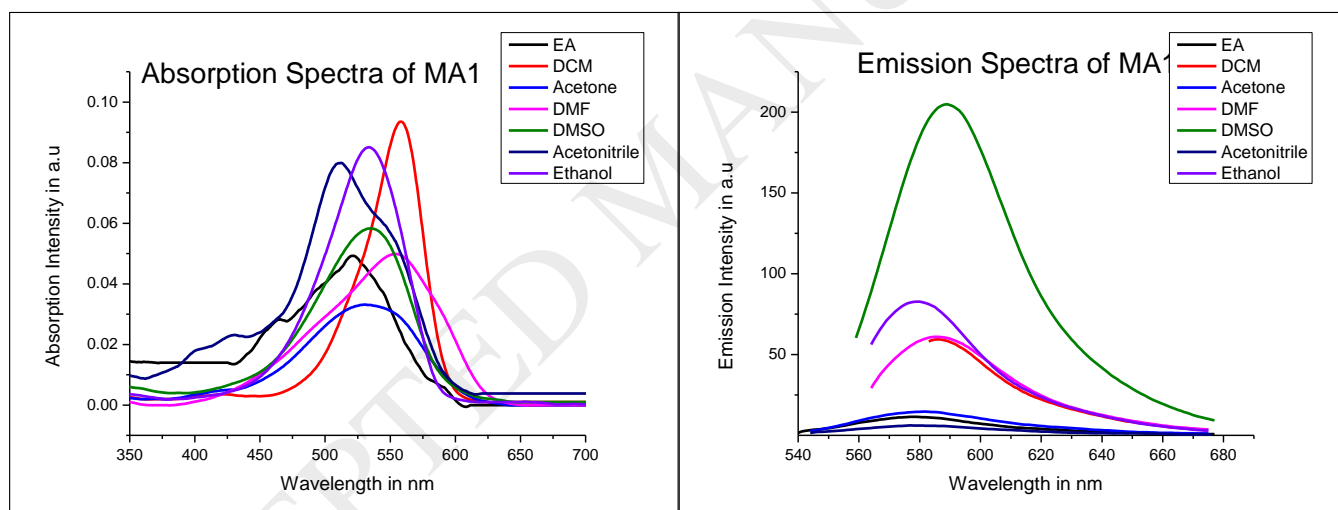


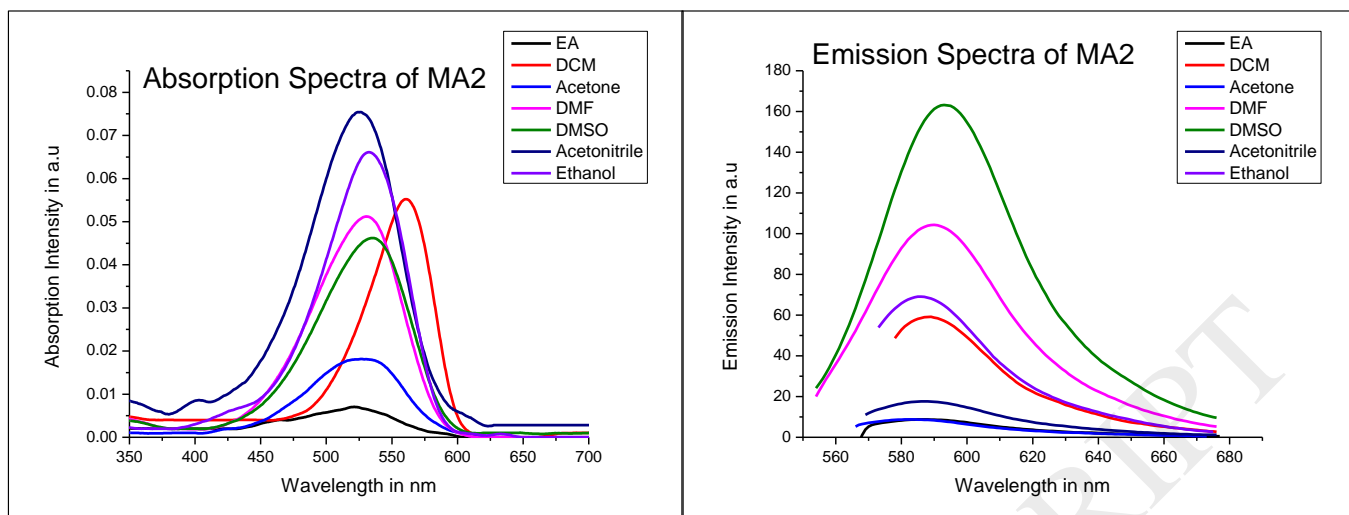
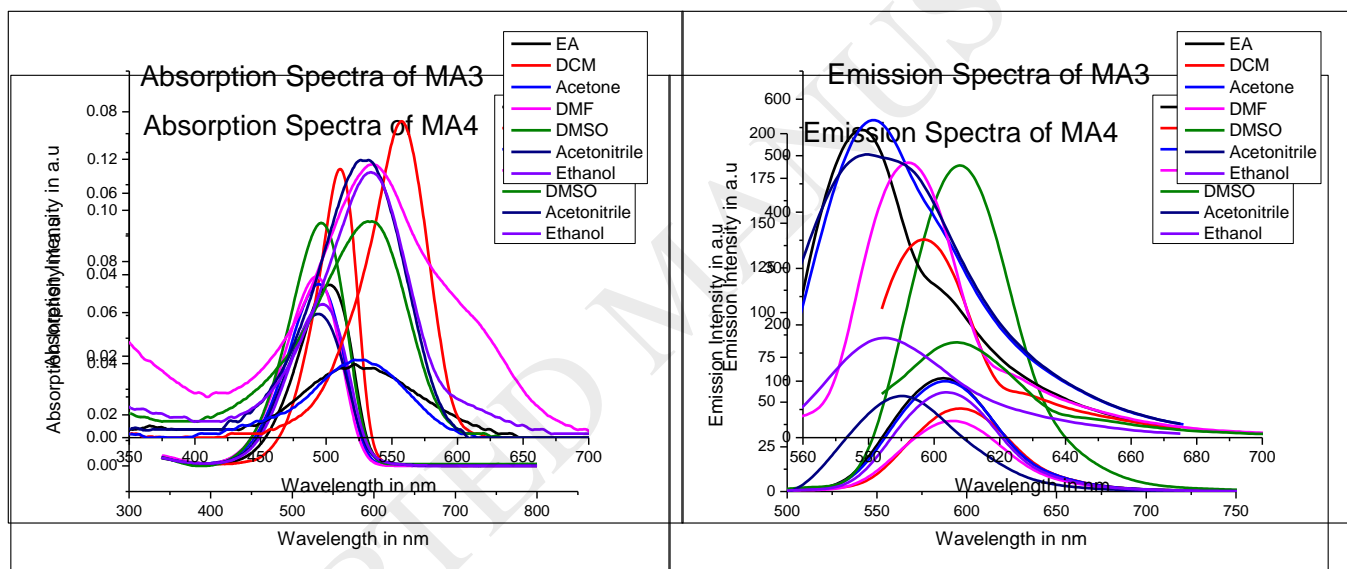
Figure 3: Absorption and emission spectra of MA2 (1×10^{-6} M)Figure 4: Absorption and emission spectra of MA3 (1×10^{-6} M)Figure 5: Absorption and emission spectra of MA4 (1×10^{-6} M)

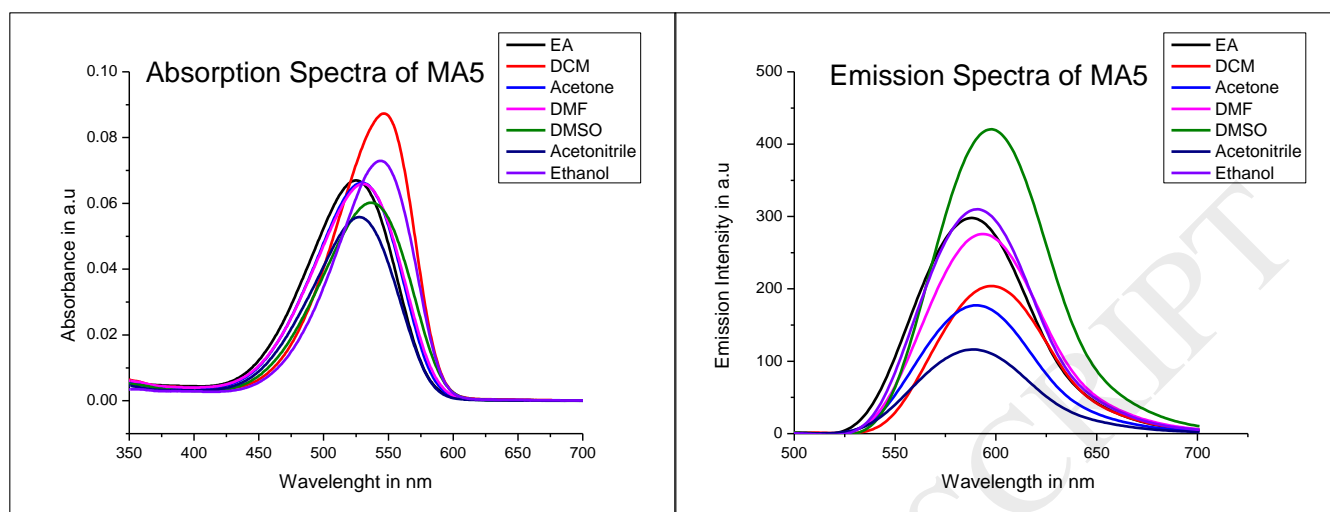
Figure 6: Absorption and emission spectra of MA5 (1×10^{-6} M)

Figure 7. Cyclic voltammogram of MA1-MA5 in acetonitrile.

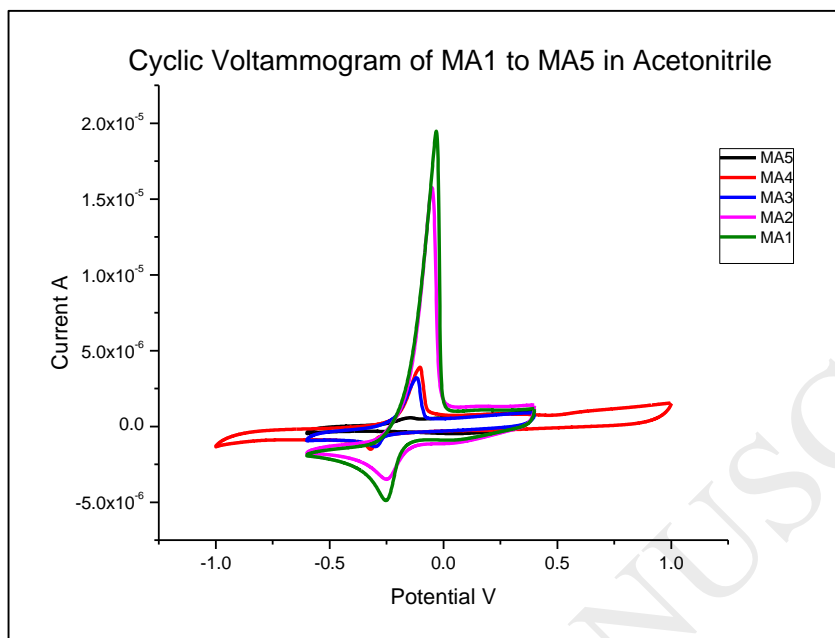


Figure 8. Comparative analysis of HOMO-LUMO energy levels obtained by Cyclic voltammetry and DFT.

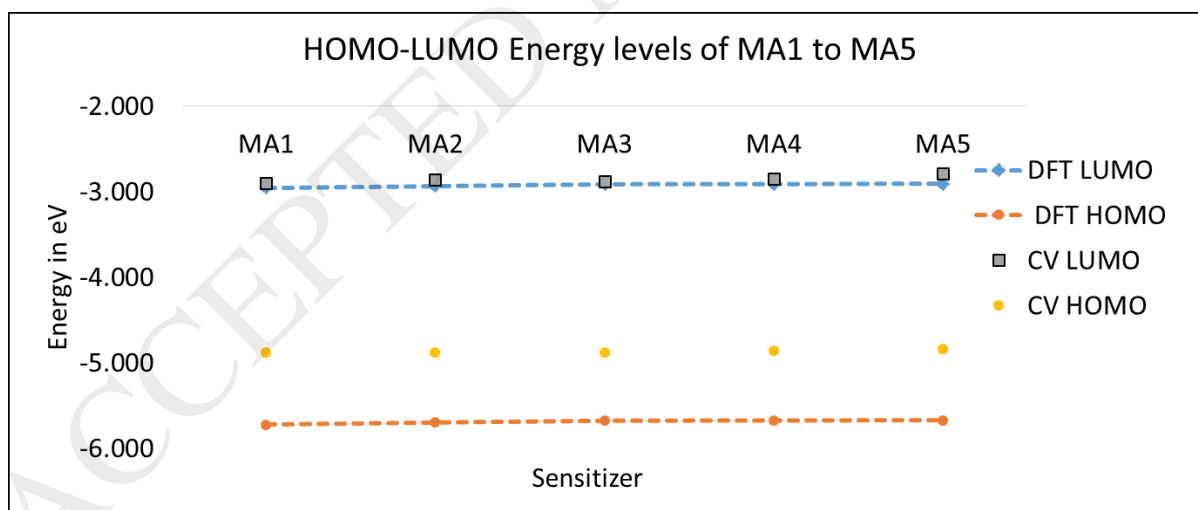


Figure 9. Pictorial presentation of electron density distribution at HOMO and LUMO in MA1 to MA5.

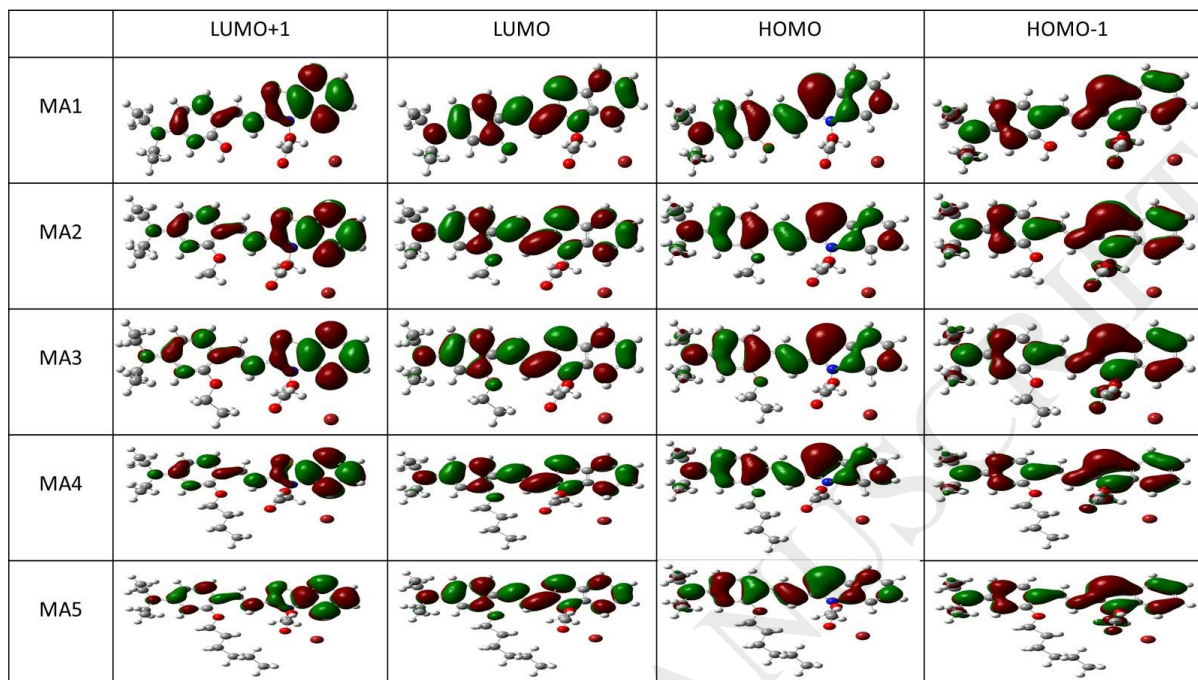


Figure 10 (a) Photovoltaic characterization (I-V spectra) MA1-MA5 and (b) Nyquist plots of DSSC devices fabricated using MA1-MA5 chromophores.

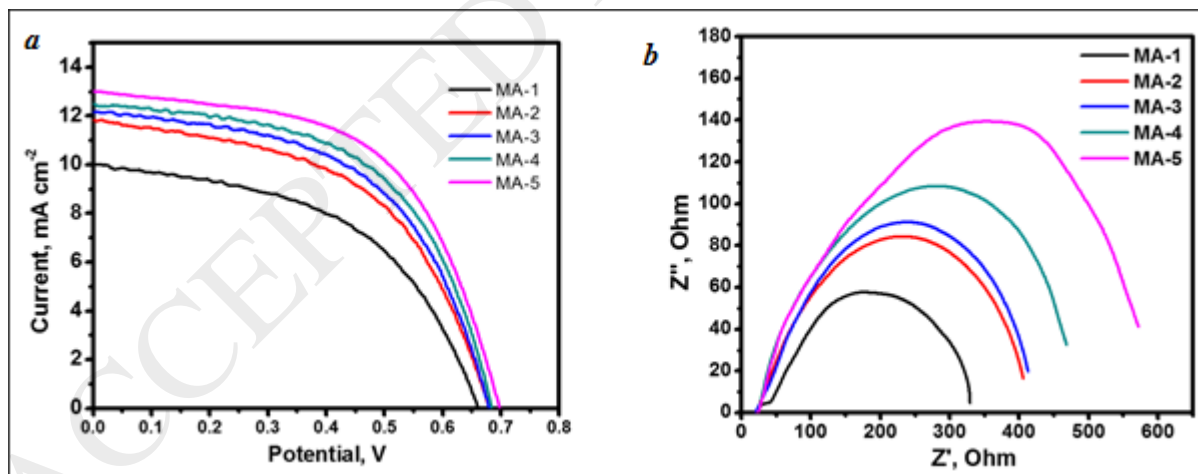


Figure 11 (a) Open Circuit Voltage Decay and (b) Electron carrier lifetime.

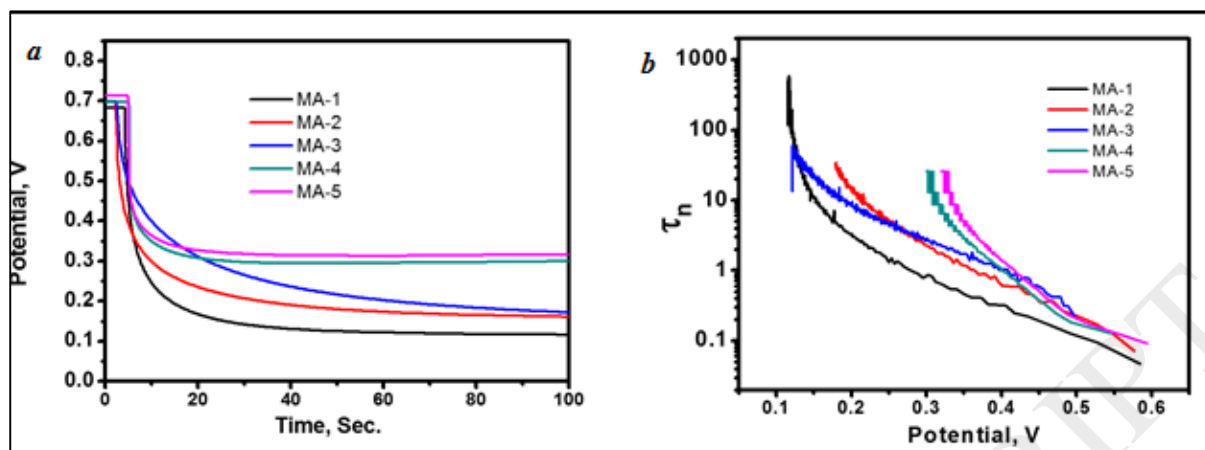
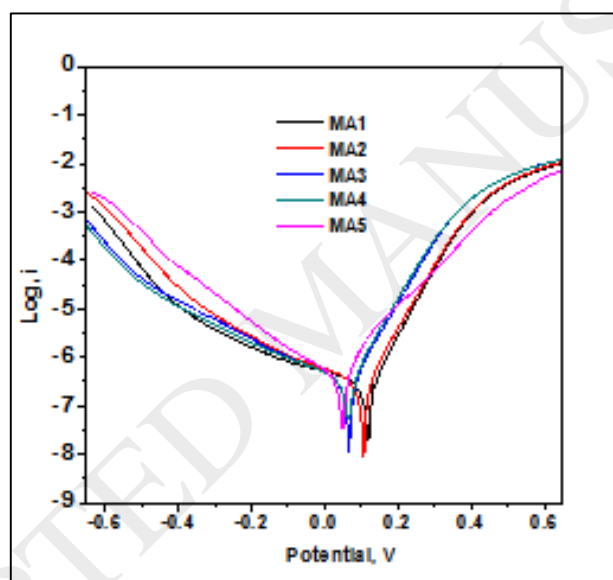
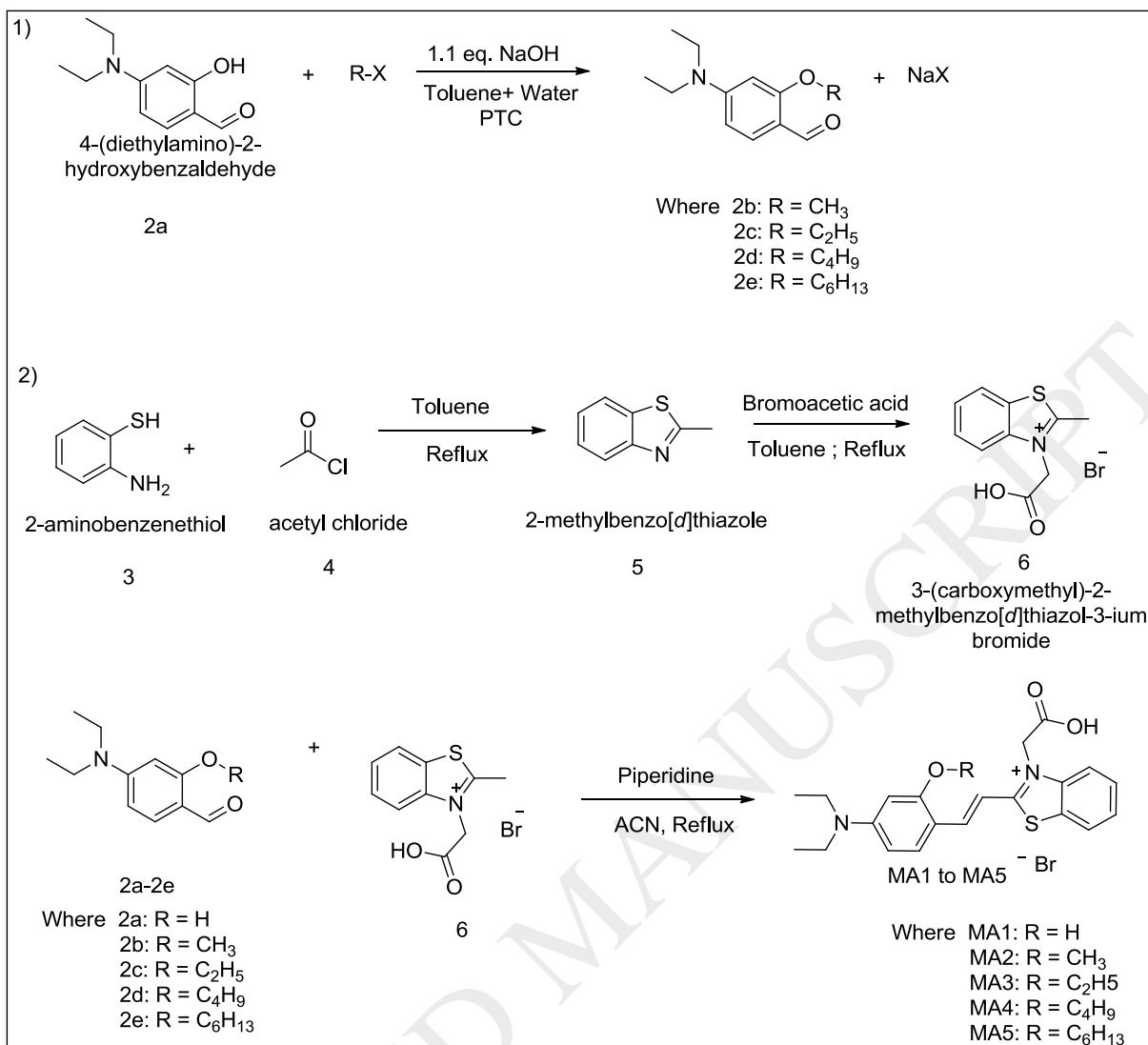


Figure 12. Tafel polarization plot.





Scheme 1: Synthesis of MA1 to MA5:

Table 1: Photo physical data for MA1

Solvent	Absorption		Emission		ϵ Max	Stokes shift		FWHM		IAC	f	Transition dipole moments for absorption	Quantum Yield
	(nm)	$\nu_a(\text{cm}^{-1})$	(nm)	$\nu_b(\text{cm}^{-1})$		$(\text{mol}^{-1} \text{cm}^{-1})$	$\Delta\nu(\text{cm}^{-1})$	(nm)	(nm)				
EA	529	18903.6	578	17301.0	49000	1602.55	49	102	4000.6	273728656.6	1.1825	11.54	0.011
DCM	560	17857.1	586	17064.8	94000	792.30	26	50	1623.4	204749027.9	0.8845	10.27	0.032
Acetone	540	18518.5	582	17182.1	33000	1336.39	42	101	3634.4	147363921.6	0.6366	8.56	0.014
DMF	558	17921.1	586	17064.8	50000	856.30	28	109	3727.3	196775638.6	0.8501	10.05	0.036
DMSO	541	18484.3	588	17006.8	58000	1477.49	47	85	3053.5	230172590.0	0.9943	10.70	0.143
Acetonitrile	516	19379.84	577	17331.0	79800	2048.82	61	87	3209.0	383864828.0	1.6583	13.50	0.009
Ethanol	536	18656.72	580	17241.4	85000	1415.34	44	71	2523.3	259317854.2	1.1206	11.31	0.052

Table 2: Photo physical data for MA2

Solvent	Absorption		Emission		ϵ Max	Stokes shift		FWHM		IAC	f	Transition dipole moments for absorption	Quantum Yield
	(nm)	$\nu_a(\text{cm}^{-1})$	(nm)	$\nu_b(\text{cm}^{-1})$		$(\text{mol}^{-1} \text{cm}^{-1})$	$\Delta\nu(\text{cm}^{-1})$	(nm)	(nm)				
EA	546	18315.0	587	17035.8	7000	1279.24	41	102	4000.6	39104093.8	0.1689	4.43	0.010
DCM	564	17730.5	589	16977.9	55000	752.57	25	58	1888.1	153081577.9	0.6613	8.91	0.038
Acetone	540	18518.5	583	17152.7	18000	1365.86	43	89	3309.3	69818410.7	0.3016	5.89	0.010
DMF	535	18691.6	590	16949.2	51000	1742.44	55	79	2910.3	178855222.7	0.7727	9.38	0.061
DMSO	541	18484.3	593	16863.4	46000	1620.88	52	83	3007.2	168040180.3	0.7259	9.15	0.112
Acetonitrile	531	18832.39	587	17035.8	75600	1796.62	56	82	3035.6	311678287.9	1.3465	12.34	0.015
Ethanol	537	18621.97	583	17152.7	66000	1469.32	46	75	2683.1	213607527.1	0.9228	10.27	0.053

Table 3: Photo physical data for MA3

Solvent	Absorption		Emission		ϵ Max	Stokes shift		FWHM		IAC	f	Transition dipole moments for absorption	Quantum Yield
	(nm)	ν_a (cm ⁻¹)	(nm)	ν_b (cm ⁻¹)		(mol ⁻¹ cm ⁻¹)	$\Delta\nu_c$ (cm ⁻¹)	(nm)	(nm)				
EA	524	19084.0	578	17301.0	18000	1782.93	54	107	3877.9	81667405.8	0.3528	6.28	0.373
DCM	558	17921.1	597	16750.4	78000	1170.73	39	53	1730.8	158474235.6	0.6846	9.02	0.235
Acetone	532	18797.0	582	17182.1	19000	1614.86	50	83	3024.5	65926846.6	0.2848	5.68	0.390
DMF	539	18552.9	592	16891.9	67000	1660.98	53	117	4008.4	392006490.7	1.6935	13.94	0.332
DMSO	538	18587.4	607	16474.5	53000	2112.90	69	83	3014.7	209245872.1	0.9039	10.18	0.125
Acetonitrile	536	18656.72	580	17241.4	68000	1415.34	44	79	2270.9	185527318.1	0.8015	10.46	0.373
Ethanol	538	18587.36	585	17094.0	65000	1493.34	47	76	2704.1	242768101.8	1.0488	10.96	0.122

Table 4: Photo physical data for MA4

Solvent	Absorption		Emission		ϵ Max	Stokes shift		FWHM		IAC	f	Transition dipole moments for absorption	Quantum Yield
	(nm)	ν_a (cm ⁻¹)	(nm)	ν_b (cm ⁻¹)		(mol ⁻¹ cm ⁻¹)	$\Delta\nu_c$ (cm ⁻¹)	(nm)	(nm)				
EA	547	18281.5	587	17035.8	70857	1245.76	40	77	2669.0	215641252.7	0.9316	10.42	0.039
DCM	559	17889.1	596	16778.5	116143	1110.56	37	57	1865.5	258380777.7	1.1162	11.53	0.026
Acetone	533	18761.7	588	17006.8	71143	1754.92	55	80	2897.2	234508242.2	1.0131	10.72	0.038
DMF	530	18867.9	592	16891.9	74000	1976.03	62	80	2914.9	244226763.6	1.0551	10.91	0.017
DMSO	535	18691.6	596	16778.5	95143	1913.07	61	80	2864.3	304721563.1	1.3164	12.25	0.121
Acetonitrile	534	18726.59	564	17730.5	59429	996.10	30	86	3117.3	207313624.0	0.8956	10.09	0.029
Ethanol	538	18587.36	589	16977.9	63286	1609.43	51	84	2982.6	213581151.3	0.9227	10.28	0.031

Table 5: Photo physical data for MA5

Solvent	Absorption		Emission		ϵ Max (mol ⁻¹ cm ⁻¹)	Stokes shift		FWHM		IAC	f	Transition dipole moments for absorption Ma (D)	Quantum Yield ϕ
	(nm)	va(cm ⁻¹)	(nm)	vb(cm ⁻¹)		$\Delta\nu$ (cm ⁻¹)	(nm)	(nm)					
EA	525	19047.6	588	17006.8	67000	2040.82	63	79	2944.2	243298439.6	1.0510	10.84	0.209
DCM	546	18315.0	598	16722.4	87364	1592.61	52	70	2413.5	265348862.5	1.1463	11.55	0.132
Acetone	529	18903.6	590	16949.2	66333	1954.44	61	79	2893.6	235503926.6	1.0174	10.71	0.120
DMF	531	18832.4	594	16835.0	65917	1997.37	63	80	2925.0	239024916.6	1.0326	10.81	0.180
DMSO	538	18587.4	598	16722.4	60167	1864.95	60	81	2874.2	211832864.9	0.9151	10.24	0.310
Acetonitrile	528	18939.39	589	16977.9	55857	1961.47	61	77	2841.3	194595152.7	0.8407	9.72	0.065
Ethanol	554	18050.54	591	16920.5	72917	1130.07	37	71	2468.3	219629030.3	0.9488	10.58	0.215

Table 6: Photophysical properties of MA1-MA5 in Acetonitrile (1.0*10⁻⁶M).

Dyes	λ_{abs}		λ_{ems}		ϵ_{max} (M ⁻¹ cm ⁻¹)	Stokes shift		TD-DFT	
	(nm)	(cm ⁻¹)	(nm)	(cm ⁻¹)		(cm ⁻¹)	(nm)	Vertical excitation (nm)	Oscillator Strength
MA1	516	19379.84	577	17331.0	79800	2048.82	61	477	1.6435
MA2	531	18832.39	587	17035.8	75600	1796.62	56	483	1.6557
MA3	536	18656.72	580	17241.4	68000	1415.34	44	480	1.6096
MA4	534	18726.59	564	17730.5	59429	996.10	30	479	1.5914
MA5	528	18939.39	589	16977.9	55857	1961.47	61	480	1.5835

Table 7: Oxidation-reduction potential of MA1-MA5 in acetonitrile obtained by cyclic voltammetry.

Sample Code	Absorption λ^a (nm)	ϵ^a (M ⁻¹ cm ⁻¹)	E_0 onset b	E_{HOMO}^c (eV)	E_g^d (eV)	E_{LUMO}^e (eV)
MA1	516	79800	-0.227	-4.873	1.973	-2.899
MA2	531	75600	-0.225	-4.875	2.014	-2.861
MA3	536	68000	-0.218	-4.882	2.001	-2.880
MA4	534	59429	-0.241	-4.859	2.015	-2.844
MA5	528	55857	-0.265	-4.835	2.050	-2.785

a Measured in acetonitrile. b Measured from cyclic voltammetry spectra. c All potentials were obtained from cyclic voltammograms. $E_{HOMO} = -(E_{onset} - (Ag/Ag^+) + 4.8)$ eV. d: calculated from UV-Visible spectra. e: Calculated from $E_{LUMO} = E_g + E_{HOMO}$.

Table 8: HOMO and LUMO energy values in eV for MA1 to MA5 in acetonitrile obtained from optimized geometry.

	MA1	MA2	MA3	MA4	MA5
LUMO+1	-0.9938	-0.9785	-0.9796	-0.9818	-1.0161
LUMO	-2.9497	-2.9323	-2.9130	-2.9113	-2.9064
HOMO	-5.7215	-5.6981	-5.6766	-5.6741	-5.6698
HOMO-1	-6.3672	-6.2948	-6.3618	-6.3642	-6.3585
Band Gap	2.7718	2.7658	2.7636	2.7628	2.7633

Table 9 Photovoltaic properties of chromophores.

Photovoltaic parameters	MA chromophore				
	1	2	3	4	5
J_{sc} (mA) ^a	10.20	11.96	12.36	12.54	13.18
V_{oc} (V) ^a	0.682	0.698	0.698	0.696	0.712
FF (%) ^a	49	50	51	53	53
PCE (%) ^a	3.40	4.17	4.39	4.62	4.97
R_{CT} (Ω) ^b	22.9	22.6	22.3	22.3	21.9
R_{rec} (Ω) ^b	192	231	246	292	340
CPE-P	0.82	0.82	0.79	0.81	0.82
β_a (mV/decade) ^c	77.4	80.5	81.4	81.8	120.9
β_c (mV/decade) ^c	449.7	368.3	307.1	392.1	318.6

^aPerformances of DSSCs were measured with 0.16 cm² working area (measurements were performed under AM1.5, 1 sun irradiation), ^bValues obtain by fitting Nyquist plot[1,2], ^c Estimated from Tafel polarization curves[3,4].

- [1] J. V Vaghasiya, K.K. Sonigara, T. Beuvier, A. Gibaud, S.S. Soni, Iodine induced 1-D lamellar self assembly in organic ionic crystals for solid state dye sensitized solar cells, *Nanoscale*. 9 (2017) 15949–15957. doi:10.1039/C7NR06128E.

- [2] T.B. Raju, J. V Vaghasiya, M.A. Afroz, S.S. Soni, P.K. Iyer, Influence of m-fluorine substituted phenylene spacer dyes in dye-sensitized solar cells, *Org. Electron.* 39 (2016) 371–379. doi:<https://doi.org/10.1016/j.orgel.2016.10.024>.
- [3] Z. Huo, C. Zhang, X. Fang, M. Cai, S. Dai, K. Wang, Low molecular mass organogelator based gel electrolyte gelled by a quaternary ammonium halide salt for quasi-solid-state dye-sensitized solar cells, *J. Power Sources.* 195 (2010) 4384–4390. doi:<http://dx.doi.org/10.1016/j.jpowsour.2009.12.107>.
- [4] K.K. Sonigara, J. V Vaghasiya, H.K. Machhi, J. Prasad, A. Gibaud, S.S. Soni, Anisotropic One-Dimensional Aqueous Polymer Gel Electrolyte for Photoelectrochemical Devices: Improvement in Hydrophobic TiO₂–Dye/Electrolyte Interface, *ACS Appl. Energy Mater.* 1 (2018) 3665–3673. doi:10.1021/acsaem.8b00444.